GENERATION AND DETECTION OF SINGLE MODE LAMB WAVES USING LASER-BASED ULTRASOUND

R.C. Addison, Jr. and A.D.W. McKie
Rockwell Science Center
Thousand Oaks, California 91358

INTRODUCTION

Lamb waves have been successfully used for the detection of defects in and on the surfaces of plate-like structures for many years [1-4]. In these applications, the Lamb waves have generally been generated and detected using angled-beam piezoelectric transducers or EMAT transducers. In certain applications where only the lowest order symmetric or antisymmetric mode was needed, laser-based ultrasonic (LBU) techniques have been used for generation and/or detection. The use of an LBU technique is attractive because of the potential for rapid inspection of large areas and because it is noncontact with large stand-off distances. The large stand-off distance is particularly attractive for the inspection of structures with elements that protrude slightly from the surface that would interfere with the movement over the surface of an angled-beam transducer or an EMAT. However, a potential difficulty is that Lamb waves are a family of guided waves that exist in plate-like structures, and a large number of modes of vibration may co-exist in a given plate thickness. An essential element in establishing the feasibility of this technique is to demonstrate that LBU techniques can select and efficiently generate a single Lamb wave mode. The selected mode will ideally have an energy distribution within the plate wall that is optimized for detection of specific defect types. Further, the dispersion characteristics of the waves depend on the specific mode and the operating point on the frequency vs wavenumber dispersion curve. The slope of the curve at the operating point of the mode selected should be nearly constant over the operating bandwidth. This implies that the group velocity is nearly constant and a pulse will maintain its compact shape as it propagates, i.e., it is nondispersive. This is especially important for the inspection of large areas where the pulse might be required to propagate over long path lengths. To obtain efficient Lamb wave generation, the mode and operating point should be selected to have a low mechanical admittance for the combination of in-plane and out-of-plane displacements produced by the thermoelastic source. Further, for an optical detector that is sensitive only to out-of-plane displacements, the mode must have a significant out-of-plane displacement at the selected operating point.

Lamb wave modes can be efficiently generated in thin metallic plates using lasers for ultrasonic generation at a single point or line[5,6]. However, this technique results in a Lamb wave source that has a broad range of both temporal and spatial frequencies and single point generation results in propagation outward from the point in all directions. For NDE applications, the ultrasonic energy must be concentrated as much as possible into a single mode that interacts optimally with the expected types of defects. Excitation of a single mode also facilitates unambiguous data interpretation. The technique for single mode generation currently being investigated requires that a series of periodically spaced line sources be projected onto a plate. The use of a line rather than a point restricts the wave propagation

Review of Progress in Quantitative Nondestructive Evaluation, Vol. 14
Edited by D.O. Thompson and D.E. Chimenti, Plenum Press, New York, 1995

direction to be perpendicular to the line. The resulting array has the effect of restricting the generated ultrasonic energy to a series of harmonically related spatial frequency bands which will be further described below. If the line sources are then periodically pulsed in time (temporally modulated), the ultrasonic energy will be further concentrated into a series of harmonically related temporal frequency bands.

METHOD FOR SINGLE MODE SELECTION

Lamb Wave Dispersion Diagram

The Lamb wave dispersion curves of the first six symmetric and antisymmetric modes in aluminum are shown in Fig. 1 calculated for a plate thickness of 1.46 mm, a longitudinal velocity of 6430 m/s, and a shear wave velocity of 3180 m/s. The dispersion curve for the bulk longitudinal wave is also shown. It is of interest to select a specific operating point on one of the mode dispersion curves which has a specified wavenumber and frequency; for example, an operating point that is at the point of intersection of Lamb wave symmetric mode 2 with the bulk wave longitudinal mode. The crossing of the longitudinal mode and symmetric mode 2 occurs at $k = 4.90$ mm^{-1} and $f = 5.01$ MHz. Although the values of λ and f given above specify the fundamental spatial and temporal frequencies of the arrays, the full spectral response must be calculated to gain insight into the other modes that might be generated.

Selection of the Mode Wavenumber

A convenient method for reducing the spatial bandwidth of the broadband wavenumber excitation provided by a single line source is to use a series of periodically spaced line sources on the plate being inspected. This will result in periodic passbands in the spatial frequency domain whose spacing and width are dependent on the spacing and number of lines in the array of sources. As an example, assume that the laser is focused to a line focus which has a Gaussian profile with a full-width half-maximum (FWHM) of 0.1 mm (Fig. 2a). This results in the broadband excitation of wavenumbers extending from 0 to more than 60 mm^{-1} (Fig. 2b). The spatial array is assumed to contain 16 elements with a

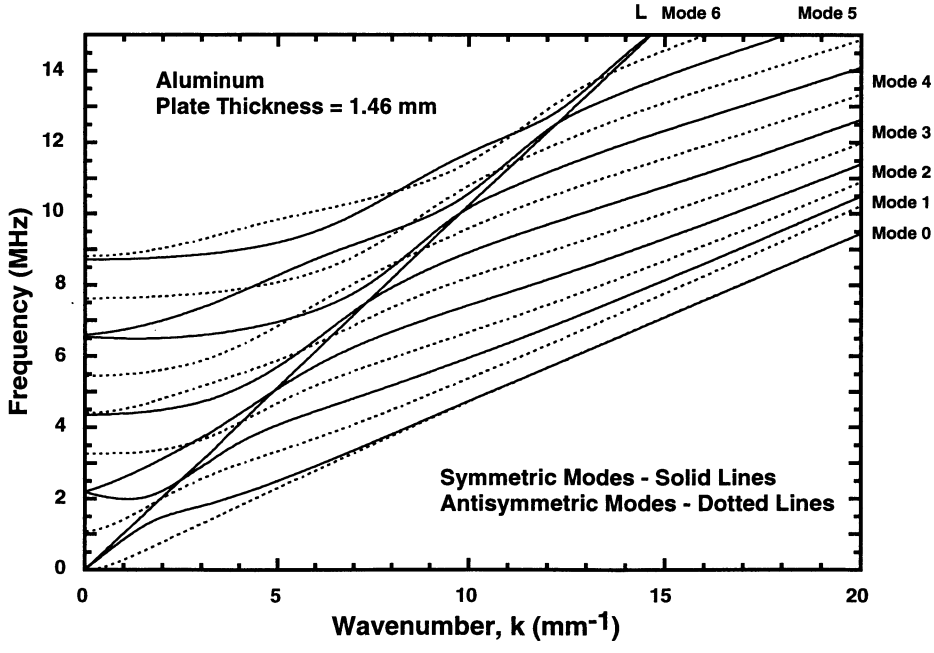

Figure 1. Lamb wave dispersion curves for a 1.46 mm thick aluminum plate.

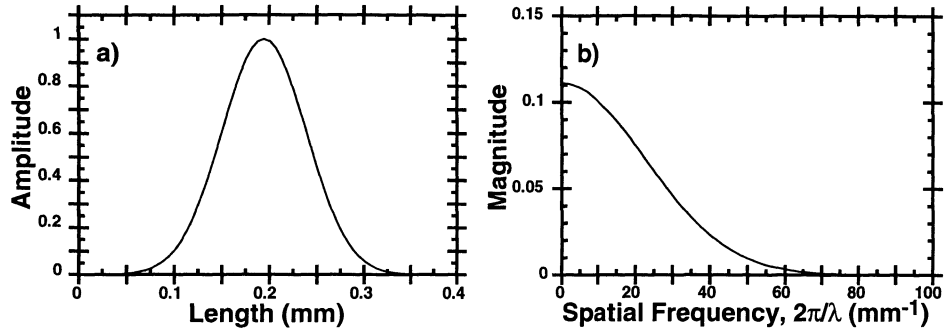

Figure 2. a) Spatial profile of focused laser beam. b) Spatial frequencies associated with this profile.

distance between them that is equal to the wavelength at the desired operating point which is $\lambda = 2\pi / k = 1.283$ mm (Fig. 3a). The spatial frequency response of the array (Fig. 3b) shows that the energy is concentrated into a series of harmonically related spatial frequency bands as expected. Note that the first full band is centered at a wavenumber $k = 4.90$ mm^{-1} as desired. The amplitudes of the other bands are contained within the envelope of the spectrum of the individual line (Fig. 2b). Thus if the line focus is made wider or narrower, this envelope will become narrower or wider in spatial frequency. The width of the spatial frequency bands produced by the array can also be narrowed by using more array elements.

Selection of the Mode Frequency

A pulse waveform produced by a Nd:YAG Q-switched laser (Fig. 4a) is used as the individual element of the temporal array. This has a FWHM of about 20 ns. The spectra of the individual pulse (Fig. 4b) extends to about 80 MHz. The temporal array is assumed to contain 4 elements with a delay time, $t = 1/5.01 \approx 0.200$ μs, between elements (Fig. 5a). The spectral response of the array (Fig. 5b) shows that the energy is concentrated into a series of harmonically related frequency bands as expected. Note that the first full band is centered at a frequency of 5.01 MHz, which is equal to the frequency of the desired operating point. The amplitude and width of these bands are controlled by the analogous quantities to those cited above for the spatial frequency bands.

Superimposing the frequency bands generated by the arrays on the Lamb wave dispersion mode graph (Fig. 1) reveals which of the other modes might be generated. The graph for the allowed Lamb wave modes in the plate having a thickness of 1.46 mm is shown in Fig. 6. Lamb wave generation is allowed only in the rectangular areas where the

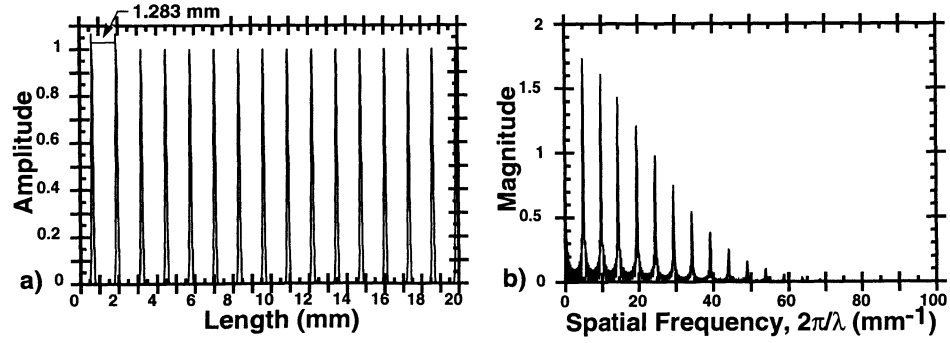

Figure 3. a) Spatial profile of an array containing 16 of the elements shown in Fig. 2a separated by 1.28 mm. b) Spatial frequency spectrum associated with the 16 element array.

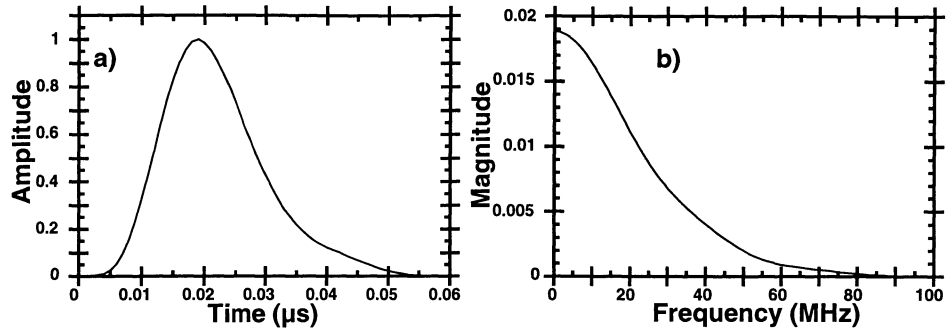

Figure 4. a) Pulse waveform produced by a Nd:YAG Q-switched laser. b) Temporal frequency spectrum of this pulse.

spatial frequency bands and the temporal frequency bands cross. Clearly the use of spatial and temporal arrays significantly restricts the allowed modes. Our chief concern is with unwanted modes within the same frequency band such as the antisymmetric modes 0 and 1 in the first frequency band. Those modes that occur in other frequency bands can be filtered from the output signals of the array if necessary.

EXPERIMENTAL RESULTS

The experiments that have been performed use a Q-switched Nd:YAG laser focused to a line to generate Lamb waves. A cw argon-ion laser also focused to a line in conjunction with a 0.5 m spherical Fabry-Pérot interferometer is used to detect the Lamb waves. A series of experiments have been performed using an aluminum plate with a thickness of 1.46 mm. During an experiment, the separation between the source and receiver is incrementally increased, with the increment selected to simulate a specific array spacing (Fig. 7). This results in a series of waveforms having increasing time delays before the arrival of the ultrasonic Lamb waves. These individual waveforms are then summed off-line in a computer so that the ultrasonic response from the simulated multiple line array of periodically spaced thermoelastic sources may be observed. The summation procedure for N element generation and detection arrays requires the collection of 2N-1 waveforms corresponding to the 2N-1 different propagation paths that can exist between the elements of the two arrays. The array response for a single generating element, G_j and an N element receiving array is synthesized by first summing each of the N waveforms, R_i, received by the detection array elements from the j^{th} generation array element.

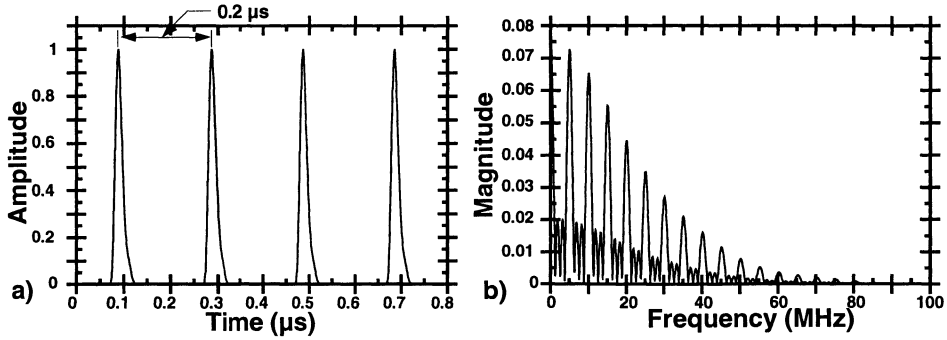

Figure 5 a) Temporal array containing 4 of the pulses shown in Fig. 4a separated by 0.200 μs. b) Temporal frequency spectrum associated with the 4 element array.

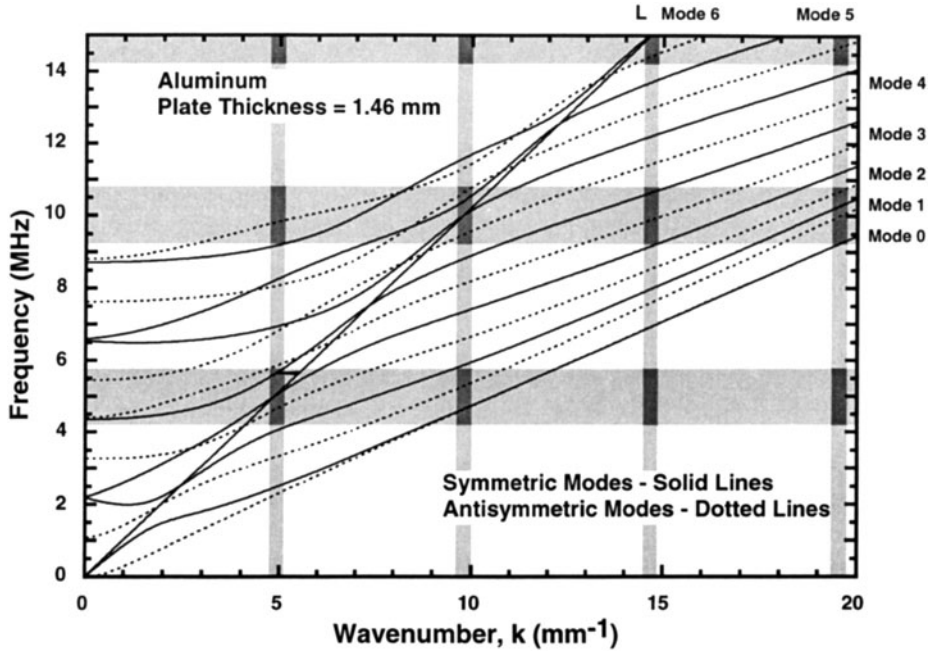

Figure 6. Lamb wave dispersion curves for a 1.46 mm thick aluminum plate with the allowed spatial frequency and temporal frequency bands superimposed.

Thus:

$$G_j = \sum_{i=1}^{N} R_i \qquad (1)$$

The N composite waveforms, G_j, resulting from this operation are summed to obtain the total waveform, W, resulting from the N element generating array and N element receiving array. Thus:

$$W = \sum_{j=1}^{N} G_j \qquad (2)$$

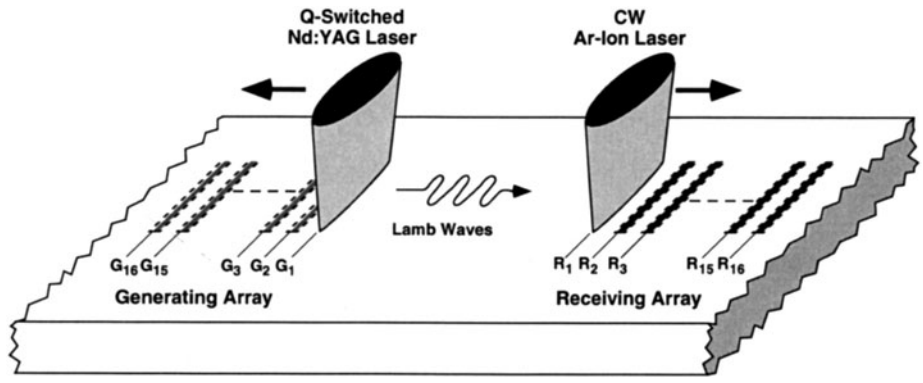

Figure 7. Schematic diagram of the experimental method used to acquire data for the synthesis of the spatial array used for restricting the spatial bandwidth of the laser beams.

Forming the array in the computer is advantageous since it enables great flexibility in array spacing and temporal modulation and thus allows the configuration to be tested and optimized before designing a laser beam array system using hardware techniques.

In the experiments, a series of ultrasonic Lamb waveforms are acquired to simulate a 16 x 16 element generating and receiving laser array. Separation between closest elements of the simulated array is ~ 23 mm, and the spacing is increased by fixed increments corresponding to the desired array spacing. The element spacing in the arrays that have been simulated ranges from 0.50 mm to 1.30 mm, with corresponding values of k for the 1st order spatial frequency band ranging from 4.8 mm^{-1} to 12.6 mm^{-1}. Figure 8a shows the temporal waveform associated with the broadband excitation of many modes by a single line source. The frequency spectrum (Fig. 8b) that is associated with this waveform is distributed over the detection bandwidth of about 1 - 15 MHz with no clearly identifiable peaks that can be associated with specific Lamb wave modes. In contrast, Fig. 9b shows the frequency spectrum resulting from the synthesized generation and detection arrays having a line spacing of 1.10 mm. Clearly the concentration of the ultrasonic energy in a few spatial frequency bands has produced the excitation of well-resolved Lamb wave modes. Of these modes, a single mode may then be preferentially selected by temporally modulating the array at the appropriate frequency. Although this has also been demonstrated with computer summation, it is not shown since digital filtering of the spectrum produced acceptable results.

Using this method of synthesizing the output of a generation and detection array, the spacing between the array elements was systematically varied from 0.50 to 1.30 mm in 0.05 mm increments. For each of the resulting 17 arrays, the peaks of the spectra were plotted in a frequency vs wavenumber diagram overlying the dispersion curves for the Lamb wave modes. In general this resulted in a series of data points that matched up with the numerically calculated dispersion curves. As shown in Fig. 9, multiple order symmetric (S) and antisymmetric (A) modes were detected as well as harmonics of the zeroth order symmetric and antisymmetric modes, nS_0 and nA_0, where n denotes the order of the harmonic. The excitation of harmonics of the zeroth order symmetric and antisymmetric modes (identified as $2A_0$, $3A_0$ in Fig. 9) causes some ambiguity in interpretation, but this can be resolved by adjusting the assumed wave number associated with the frequency peak to be a higher harmonic of the spatial frequency spectrum. When the correct order for the wavenumber is used, the points align closely with the coalesced curves for the S_0 and A_0 modes.

The peaks in the frequency spectrum were tabulated for the 17 different arrays. These results are shown graphically in Fig. 10, which also shows the numerically calculated dispersion curves for both symmetric and antisymmetric modes. Figure 10 shows very good agreement between the experimental and theoretical data. The zeroth order symmetric and antisymmetric modes were the only ones detected over the full wavenumber range. There is a region over which the 1st order symmetric mode was not detected between the wavenumber

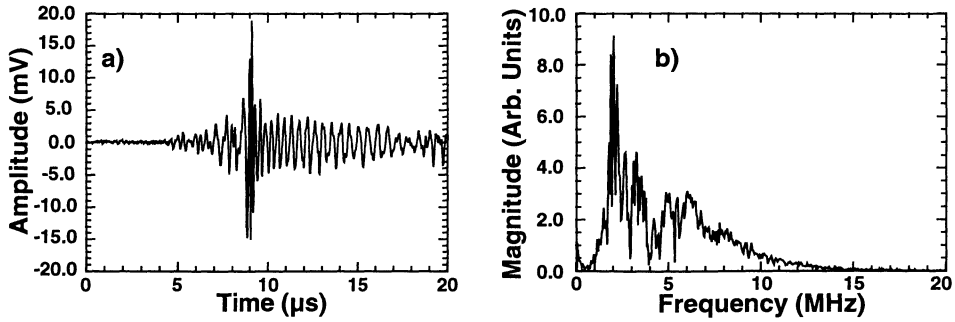

Figure 8. a) Temporal waveform resulting from broadband excitation of multiple Lamb wave modes. b) Frequency spectrum associated with this waveform.

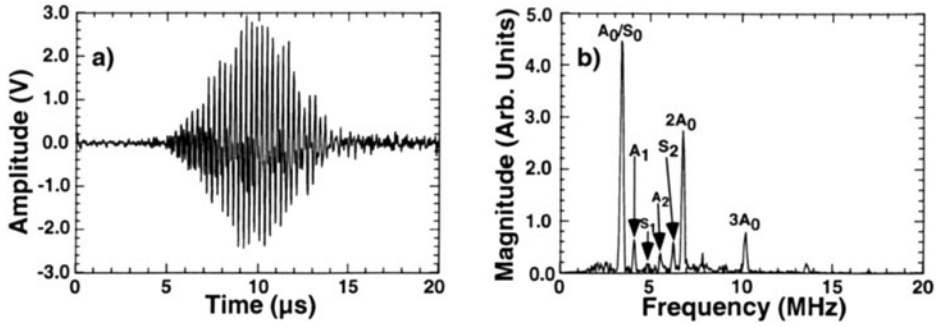

Figure 9. a) Temporal waveform obtained form a spatial array with an element separation of 1.10 mm. b) Frequency spectrum associated with this waveform.

values 6.0-7.3 and the other modes, A_1, S_2, and A_2 were not detectable at the higher wavenumbers. In some instances, the Lamb wave mode of interest was not detectable because it was masked by the large amplitude harmonics of the antisymmetric mode. In other instances, the admittance for a particular mode may have been high, resulting in inefficient excitation. This result demonstrates that LBU techniques can be used to generate both symmetric and antisymmetric Lamb wave modes at least up to mode 2. Any of the modes shown in Fig. 10 can be isolated by filtering the output signal, W, that is obtained from the synthesized arrays. As an example, the S_2 mode for an array spacing of 0.85 mm is shown in Fig. 11. This is a compact pulse with a relatively narrow bandwidth that can be used for various NDE applications such as detection of cracks and thinning of plates caused by corrosion.

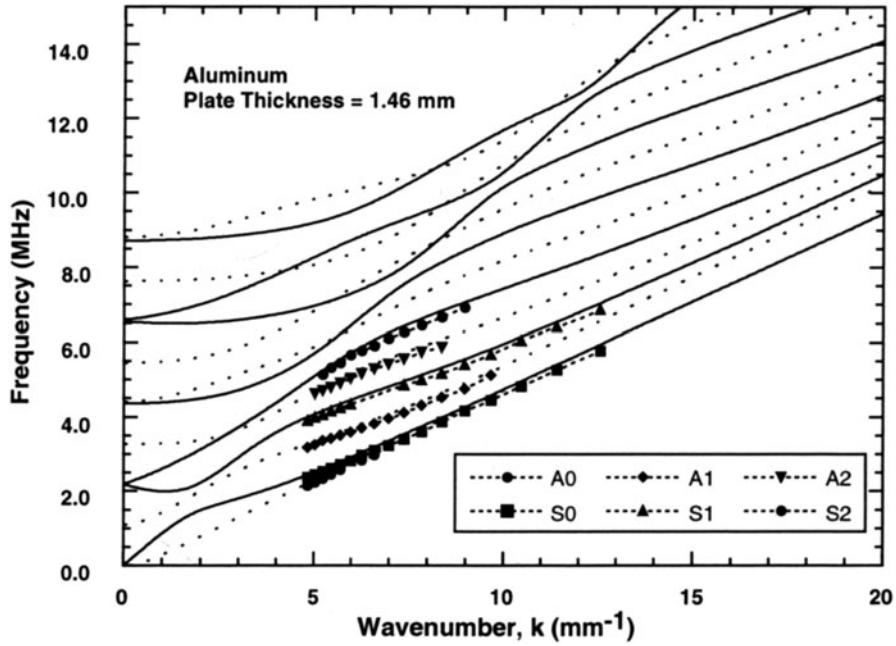

Figure 10. Lamb wave dispersion curves for a 1.46 mm thick aluminum plate overlaid with the data points obtained from experiments using 17 different array element spacings ranging from 0.50 - 1.30 mm.

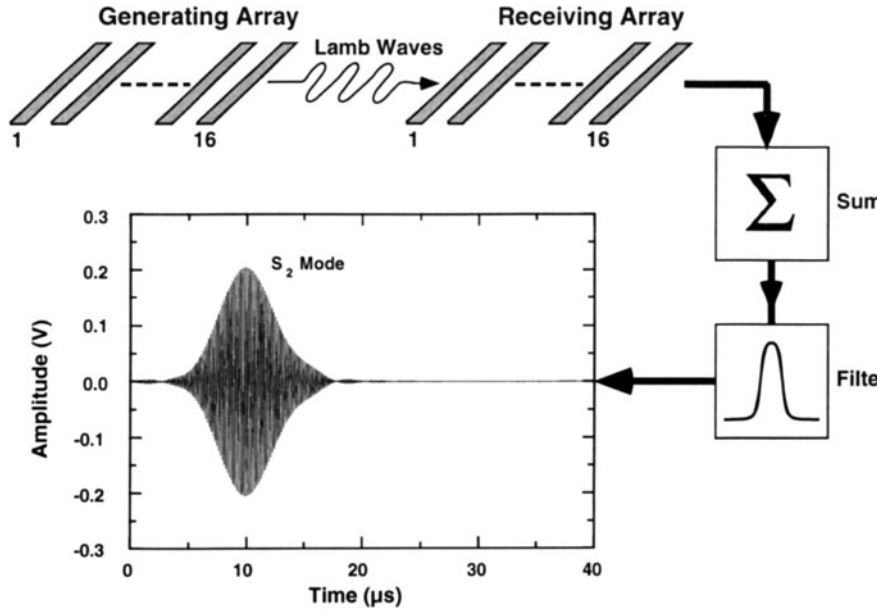

Figure 11. Temporal pulse resulting from isolation of the S_2 Lamb wave mode obtained with an array element spacing of 0.85 mm.

CONCLUSIONS

In many situations, the use of a laser to generate and detect Lamb waves results in a source that is broadband in both temporal and spatial frequencies which causes the simultaneous excitation of many modes. Although the zeroth order modes can be isolated by judicious choice of the frequency or the plate thickness, this does not permit selection of the optimum Lamb wave mode for many NDE applications and causes difficulties in data interpretation. This paper has demonstrated that the restriction of the spatial and temporal bandwidth by the use of arrays permits the generation and detection of a single Lamb wave mode. The generation of both symmetric and antisymmetric modes of zeroth through second order was demonstrated in an aluminum plate. Excellent agreement was obtained between the frequency and wavenumber of these modes and the numerically calculated Lamb wave dispersion curves for aluminum. These results led to the feasibility of using LBU techniques to select and generate a single mode Lamb wave.

ACKNOWLEDGMENTS

This work was supported by The Gas Research Institute and the Rockwell Internal Research and Development program. We thank T.A. Gray for supplying the program used for calculating the Lamb wave dispersion curves.

REFERENCES

1. D.C. Worlton, Non-destructive Testing 15, 218 (1957).
2. D.F. Ball and D. Shewring, Non-destructive Testing 9, 13 (1976).
3. S.I. Rokhlin and F. Bendec, J. Acoust. Soc. Am. 73, 55 (1983).
4. R.B. Thompson and D.O. Thompson Proc. IEEE 73, 1716 (1985).
5. R. J. Dewhurst, C. Edwards, A. D. W. McKie, and S. B. Palmer, Appl. Phys. Lett. 51 1066 (1987).
6. D. A. Hutchins, K. Lundgren and S. B. Palmer, J. Acoust. Soc. Am. 85, 1441 (1989).